GNSS Interference Source Localization Using ADS-B data

Zixi Liu, *Stanford University*
Sherman Lo, *Stanford University*
Todd Walter, *Stanford University*

BIOGRAPHY

Zixi Liu is a PhD candidate at the GPS Laboratory at Stanford University. She received her B.Sc. degree from Purdue University in 2018 and her M. Sc. degree from Stanford University in 2020.

Sherman Lo is a senior research engineer at the GPS laboratory at Stanford University.

Todd Walter is a Professor of Research and director of the GPS laboratory at Stanford University.

ABSTRACT

Automatic Dependent Surveillance – Broadcast (ADS-B) reports from aircraft have been examined by several groups for their capabilities to identify regions affected by radio frequency interference (RFI) [1] [2] [3]. RFI events that happen near airports could cause denial of GNSS based landings for aircraft and create a severe impact on the safety of aircraft operation during some vulnerable segments. Therefore, it is important to rapidly localize any GNSS interference sources and identify the geographical impact area. Using already existing aircraft reports of position from ADS-B is a highly desirable approach that could rapidly and inexpensively be implemented nationwide or even globally.

This project has two main objectives. First, we developed a method of interference source localization which is applicable for different types of interference source using ADS-B data. Specifically, the mathematical model was designed without prior knowledge on the power level of RFI sources, making this factor as parameter to identify. Although this approach increases complexity, it allows our models to be more flexible and general. Second, we built an interference event simulator which generates ADS-B data from simulated aircraft flight tracks that may be affected by simulated RFI events. By building this simulator, we can then test our models for different scenarios including multiple jammers. Identifying and obtaining real-world ADS-B data from these types of events is difficult. Therefore, we rely on simulated data to better test our models for these special cases. To make the simulated data reasonable, our simulator also adds noise and includes erroneous outputs that we have observed during the investigation of real-world interference events.

I. INTRODUCTION

ADS-B is a satellite-based surveillance system used by commercial aircraft and was made mandatory in Europe and the U.S.A. by 2020 [4]. It broadcasts position and velocity messages based on positions from certified GNSS based position estimates. These messages are transmitted every 0.4 – 0.6 sec through Mode-S Extended Squitter on the 1090 MHz frequency band. Nowadays, several companies and associations provide access of ADS-B data, such as The OpenSky Network [5] which has a ground network of ADS-B sensors/receivers over the world. Therefore, the ubiquity and openness of ADS-B provides an available and widespread source of GNSS information from aircraft and a means to identify and localize RFI sources.

GNSS provides the basis for safety-of-life service in aviation. RFI source can disrupt aircraft operations and result in unavailability of service including approach and landing. This sudden loss of navigation can be monitored through ADS-B reports on the ground side. Figure1 shows how interference event can affect ADS-B outputs.

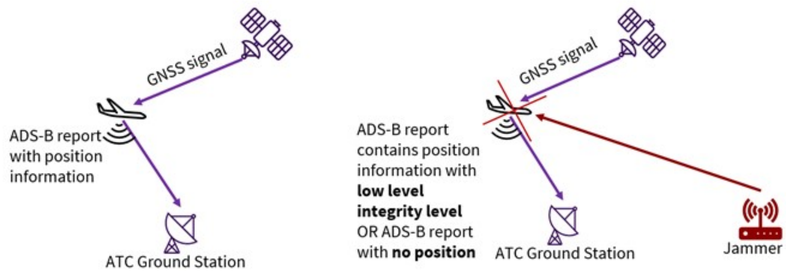

Figure 1: Impact of interference event on ADS-B performance

Several groups have investigated the use of ADS-B on detection or localization of GNSS interference events. Aireon is able to provide alerts of potential GPS interference events by monitoring change of Navigation Accuracy Category–Position (NACp) parameter from ADS-B message [1]. EUROCONTROL has investigated the use of ADS-B to determine GNSS affected regions in the eastern Mediterranean. They developed a grid probability model, based on ADS-B trajectory gaps, to identify possible location of the RFI source [6].

This project expanded upon some of the concepts developed in prior research [3] [7] and developed new approaches for RFI source localization using ADS-B data. The overall concept is as following: given an airspace with suspected interference event, assume that the RFI source could be anywhere on the ground with unknown power level, at each possible location combined with different power level, We estimate how the assume jammer could affect surrounding aircraft, and then we calculate the probability of our estimated result matching with true result based on ADS-B data collected from that airspace.

II. APPROACHES

1. Information from ADS-B data

According to DO-260B [8], Navigation Integrity Category (NIC) is a parameter in ADS-B airborne position message which indicates the integrity level of current position information. This parameter is related to the Required Navigation Performance (RNP) information from the GNSS receiver. It indicates the size of the containment radius of the current reported position. Imagine drawing a circle centered at reported position, the actual position has 99.999% probability of being somewhere within the circle. Therefore, the smaller the containment radius is, the higher the accuracy the information has. Table1 shows the size of the containment radius corresponding to each possible NIC value.

Table 1: NIC value and corresponding size of containment radius

NIC	Containment Radius
0	Unknown
1	$R_c < 37.04$km (20nm)
2	$R_c < 14.816$km (8nm)
3	$R_c < 7.408$km (4nm)
4	$R_c < 3.704$km (2nm)
5	$R_c < 1852$m (1nm)
6	$R_c < 1111.2$m (0.6nm)
	$R_c < 926$m (0.5nm)
	$R_c < 555.6$m (0.3nm)
7	$R_c < 370.4$m (0.2nm)
8	$R_c < 185.2$m (0.1nm)
9	$R_c < 75$m
10	$R_c < 25$m
11	$R_c < 7.5$m

Given a suspected RFI event, one way to check whether or not an aircraft has been jammed at one position is to check the

ADS-B equipment performance requirements defined in Title 14 of the Code of Federal Regulations (CFR) Part 91 [4]. One of the requirements is that, under normal circumstances, the aircraft's NIC value must be ≥ 7 (containment radius less than 0.2 nautical miles). Therefore, if there exist multiple data points with NIC values less than 7, that could be a clear indication of existence of RFI sources. Our previous studies in characterizing ADS-B performance during interference events indicated that this rule is a quite reasonable means of identifying RFI events [3].

2. Mathematical model for RFI event

Once we have identified a region with ADS-B position points with low NIC values, we can calculate the jamming power received at each location using following equations.

a) Signal line of sight

The first step is to check if current aircraft position is within the radio line of sight(LOS) of the RFI source.

$$RHR_{[km]} = 4.12[\frac{km}{\sqrt{m}}] * (\sqrt{h_{[m]}} + \sqrt{a_{[m]}}) \tag{1}$$

where "RHR" is the horizontal distance between jammer and aircraft, "h" is the ground elevation/height of jammer in meters and in this project we assumed h = 0, "a" is the critical altitude of aircraft in meters. If the altitude of the aircraft is lower than the critical altitude, then the aircraft is outside line of sight of the jammer. In other words, the jammer will not be able to impact the flight and vice versa. Figure 2 illustrates this equation.

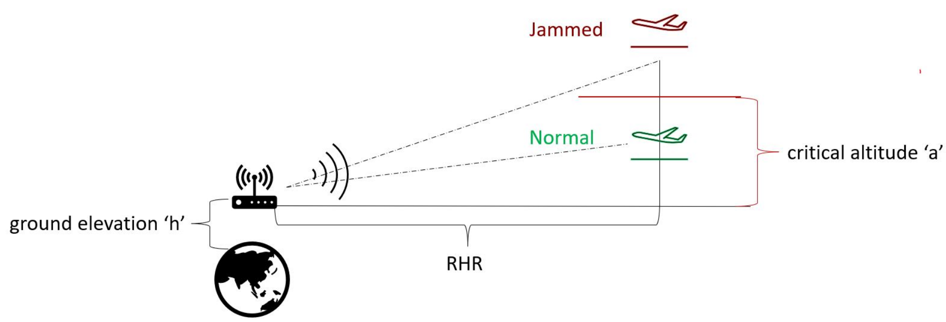

Figure 2: Implementation of line of sight equation

b) Power level

Once the aircraft is within the line of sight of the jammer, we then consider the power level of the jammer. In the analysis in the paper, we assumed that the RFI source has omnidirectional radiation with continuous transmission, and no additional significant masking caused by other obstacles. Therefore, the impact region of a RFI source can be illustrated as in Figure 3. "r_i" is the imaginary effective impact radius of the jammer, "d" is the distance between the aircraft and the jammer. When the distance between the jammer and the aircraft is smaller than the effective impact radius, given that the aircraft is within the line of sight, the aircraft should be affected by the jammer.

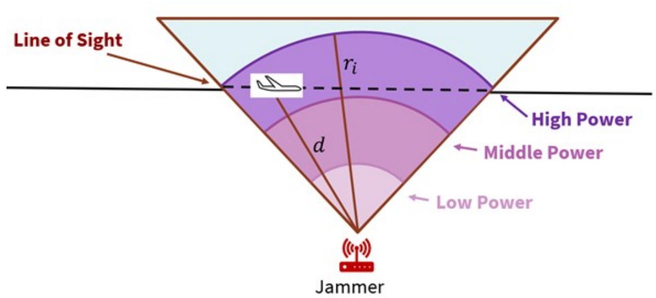

Figure 3: Representation of impact radius as function of jammer power level

c) *Free space path loss*

For position points that are within line-of-sight and the impact region of the jammer, we then calculate the amount of jamming power received at each point. We use the free space path loss equation [9] which shows the power loss of a signal from the transmitter to the receiver in a space without signal blockage:

$$P_L = \frac{P_t}{P_r} = (\frac{4\pi d}{\lambda})^2 \frac{1}{G_t G_r} \tag{2}$$

where P_r is the power received in watts, P_t is the power transmitted in watts, P_L is the power loss ratio, λ is the transmitted signal wavelength in meters, d is the distance between transmitter and receiver in meters, G_t, G_r are the transmit and receive antenna gain.

In this project, we treat RFI source as the transmitter and the GNSS receiver on the aircraft as the receiver. Assuming G_t and G_r are both equal to 1, if we know the distance d between the aircraft and the jammer, we could calculate P_r which is the amount of jamming power received at one position point.

3. Relating NIC with Received Power(P_r)

In this project, we tried different test cases about jammer power and jammer location. For each scenario, we calculate jamming power received by each aircraft and we can compare the estimated result with true result based on NIC values collected from ADS-B data.

In order to do that, we need to find out the relation between NIC and Pr based on empirical data. The real-world data we collected contains ADS-B data from interference events happened in Cypriot airspace [10] and the estimated true possible location of the interference source has been identified by C4ADS using satellite data [11]. Figure 4 is a sampled plot showing the air traffic in selected airspace on 12/14/2020. The color of each point represents the corresponding NIC value. The possible location of interference source identified by C4ADS is marked by the pink dot. Since we have information about aircraft positions, NIC values, and true location of the jammer, once we estimated the transmitted jamming power(P_t), we can then calculate P_r values of each point and find a relation between P_r and NIC.

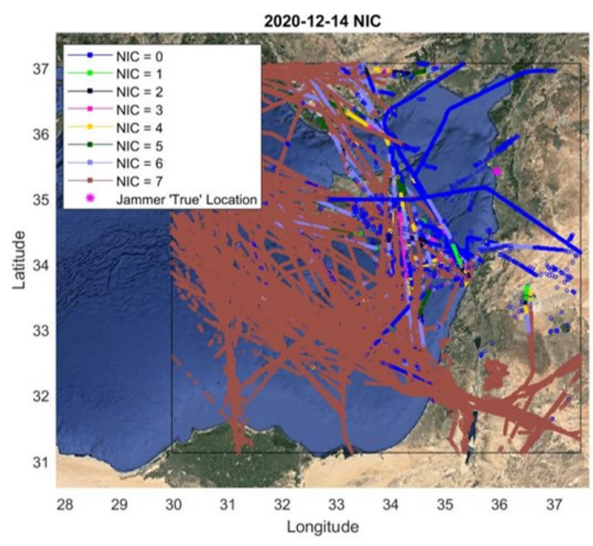

Figure 4: Top view of air traffic in selected airspace

The first step is to separate aircraft position points into groups based on levels of jamming impact which is indicated by P_r. From equation [9], P_r is proportional to the inverse of the distance squared, therefore, grouping data points with similar distances allows us to group similar P_r. Figure 5 shows the grouping result, the legend on the left shows the color and the averaged distance of each group, the legend on the right shows the averaged P_r of each group. During the calculation of P_r values, we also estimated the transmitted power(P_t) from the jammer. We started by assuming a C/No tracking threshold of 25[dB-Hz], then according to the book Understanding GPS/GNSS: Principles and Applications [12], the maximum tolerable jamming power at the aircraft would be $P_r \approx -115$[dBW]. We then calculated the P_t that would result in $P_r \geq -115$[dBW] for affected points. This leads to our estimate of $P_t = 1000$[W]. Noticed that points that are in blue, red, green, black, and pink correspond to points with NIC values less than 7 and mostly equal to 0 in Figure 4, which were under RFI impact. In addition, these points have P_r values larger than or equal to -115[dBW]. Therefore, using $P_t = 1000$[W], the corresponding affected region aligns with what is observed from ADS-B data.

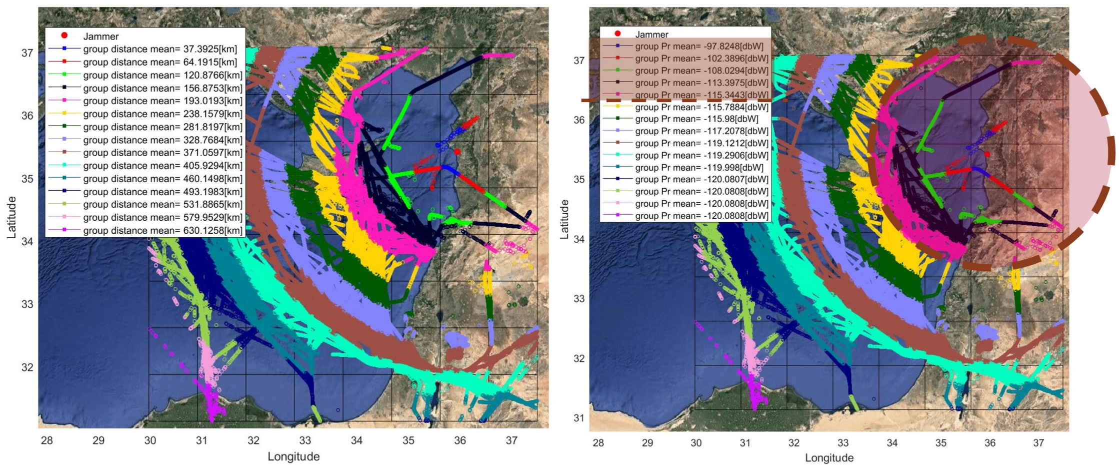

Figure 5: Separate aircraft position points into different groups

The second step is to generate the probability mass function(PMF) of NIC values for each P_r group. For calculation simplicity, we set all values of NIC > 7 to NIC = 7. This is because NIC > 7 does not provide additional information about interference event, as long as NIC values are not less than 7, we will treat them as points that are not affected. In order to calculate the PMF for each group, we need to find out $P(\text{NIC} = \text{nic}_i)$ with $\text{nic}_i \in [0, 1, 2, ..., 7]$. This can be calculated by dividing numbers of points with NIC value equals to nic_i by the total numbers of points in the group. For instance, in the group of blue points with averaged P_r = -97[dBW], NIC values of all data points are equal to 0. Therefore, $P(\text{NIC} = 0) \approx 1$, $P(\text{NIC} = 1) \approx 0$, ..., and $P(\text{NIC} = 7) \approx 0$. To avoid extreme cases, we approximate probability of 0 as 0.01 and probability of 1 as 0.99. Within each color group, the probability mass function sums to 1. Figure 6 shows the PMF of the group of pink points(averaged $P_r \approx -115$[dBW]). We performed above calculation for points that are within line-of-sight and points that are outside line-of-sight separately, because points that are above the line of sight are much more likely to be jammed than those below.

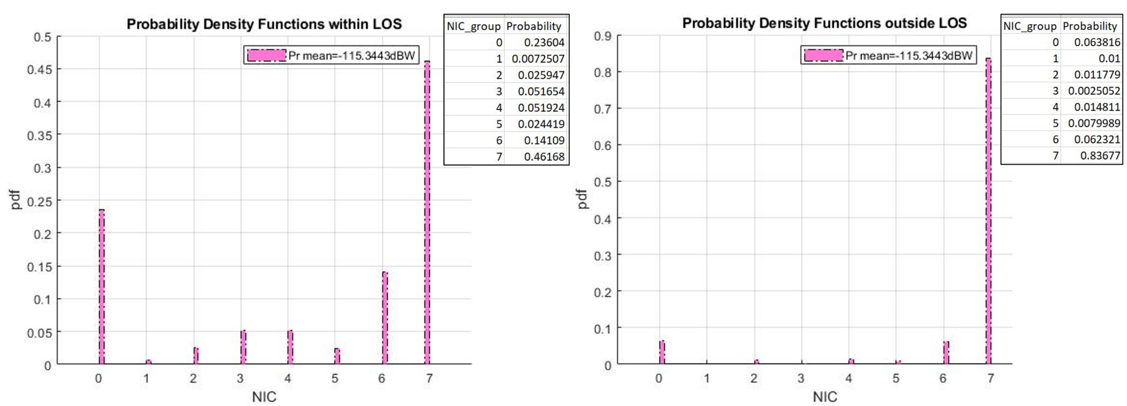

Figure 6: Probability mass function of NIC for points with $P_r \approx -115$[dBW]

Figure 7 shows the PMFs of each group with side-by-side bars on same plot, legend shows the color and averaged P_r value of each group. PMFs in the plot on the left are applicable for points that are within line-of-sight and PMFs in the plot on the left are applicable for points that are outside line-of-sight

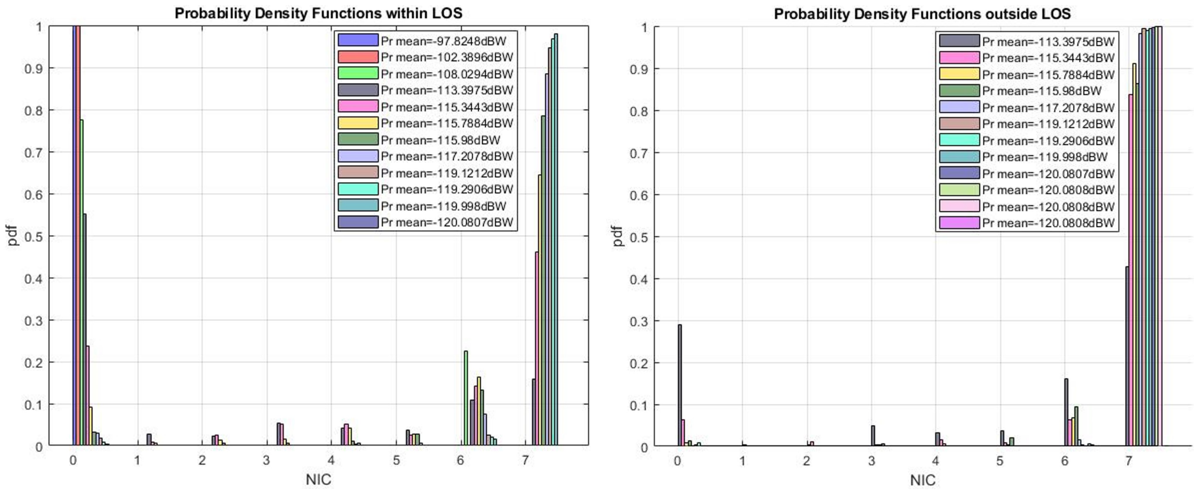

Figure 7: Probability mass function of NIC for different groups of position points

III. CALCULATION

Now that we understand the relation between NIC and P_r, we can calculate the probability of each scenario being true and return the one that has highest probability.

1. Create all possible scenarios

The first step is to enumerate all possible scenarios to assess. These scenarios are meant to span the possible interference situation and the goal is to find the scenario (jammer power and location) that has the highest probability given the data. This process can be implemented by performing an iterative grid search which is illustrated in Figure 8. Different jammer locations are placed at discrete grid locations on the ground, each representing one possible location of the jammer. Discrete power levels are also evaluated which is illustrated as effective jamming radius as depicted in Figure 8.

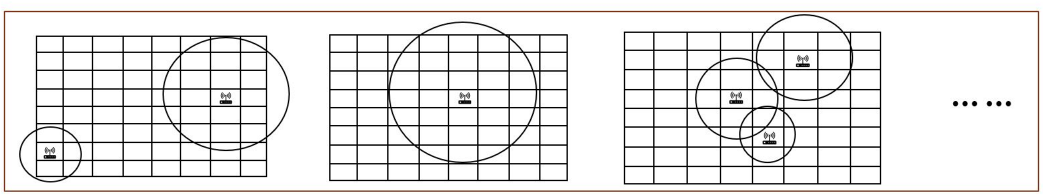

Figure 8: Create all possible scenarios within selected airspace

2. Adjusting PMFs for each scenario

The next step is to adjust the probability mass function based on an assumed P_t value at each scenario. The PMF generated in section II.3 uses $P_t = 1000[\text{W}]$ which is treated as a reference jamming power $P_{t_{ref}}$. For each scenario, although the value of P_t is different, we can still use the same probability distribution curve as if $P_t = P_{t_{ref}} = 1000[\text{W}]$, but the way we determine which group/ PMF curve one point belongs to has changed. According to free space path loss equation, if the transmitted power changes from P_t to $P_{t_{ref}}$, to receive same amount of power P_r, the distance from aircraft to the jammer should decrease by $\frac{d}{d_{ref}} = \sqrt{\frac{P_t}{P_{t_{ref}}}}$. That means if we say group one has averaged distance of d in reference scenario $P_{t_{ref}} = 1000[\text{W}]$, then for current scenario P_t, group one has averaged distance of $\sqrt{\frac{P_t}{P_{t_{ref}}}}d$. For instance, if jamming power changes from 1000[W] to 100[W], then effective impact distance shrinks by $\sqrt{\frac{1}{10}}$.

3. Bayes estimation

The final step is to apply Bayes Rule to estimate the probability of each scenario being true.

Step1: Among entire airspace, collect ADS-B data, assuming we have m data points, each with information (latitude$_i$, longitude$_i$, altitude$_i$, nic$_i$), overall forming vectors of $\hat{\text{Lat}}$, $\hat{\text{Lon}}$, $\hat{\text{Alt}}$, $\hat{\text{Nic}}$ each $\in R^{(m,1)}$.

Step2: Form n numbers of possible scenarios, each scenario contains information about jammer (x_j, y_j, z_j, P_{t_j}).

Step3: Select j_{th} scenario out of all scenarios and calculate:

$$P(\text{scenario}_j|\text{NIC} = \hat{\text{Nic}}) = \frac{P(\text{NIC} = \hat{\text{Nic}}|\text{scenario}_j)P(\text{scenario}_j)}{P(\text{NIC} = \hat{\text{Nic}})} \tag{3}$$

Where we could assume that $P(\text{scenario}_j)$ which is the probability of each scenario itself being true and $P(\text{NIC} = \hat{\text{Nic}})$ which is probability of having current overall picture of NIC values in selected airspace are the same among all scenarios. Then finding the scenario with maximum $P(\text{scenario}_j|\text{NIC} = \hat{\text{Nic}})$ is equivalent to finding the one with maximum $P(\text{NIC} = \hat{\text{Nic}}|\text{scenario}_j)$.

$$P(\text{NIC} = \hat{\text{Nic}}|\text{scenario}_j) = \prod_{i=1}^{m} P_i(\text{nic} = \text{nic}_i|\text{scenario}_j) \tag{4}$$

Where each $P_i(\text{nic} = \text{nic}_i|\text{scenario}_j)$ is the probability of each position point with NIC value = nic$_i$ being true under current j_{th} scenario. This value can be found from probability mass function we generated before.

Step4: Normalize $P(\text{scenario}_j|\text{NIC} = \hat{\text{Nic}})$ among all scenarios such that probabilities of all scenarios sum to 1. Then the one with highest probability shows the possible location and power level of the RFI source.

IV. RESULTS AND ANALYSIS

In this project, we tested our algorithm using data from both real interference events and simulations. This helps us to check if there is any logistic problems in our approaches for ideal cases, as well as to check the robustness of our models in real cases.

1. Real cases

The real-world data we used in this project is ADS-B data from interference events happened in Cypriot airspace shown in Figure4. To illustrate the results from different scenarios, assuming there is only one jammer with possible transmitted power ranging from 1 watt to 1000 watts and the jammer could be located at the center of any grid. Figure9 shows probability of each scenario. From left to the right shows jammer with P_t from 1 watt to 1000 watts. The probability of having a jammer at each location is shown in green text. The location with highest probability at each power level is shown in red text. The effective impact region corresponding to each power level is presented as red circle. Noticed that as power level increases, in other words, as size of impact region becomes larger, the most probable jammer location changes from middle right to the upper right corner. This tendency of moving to the upper right corner matches with our sampled data in which most of the jammed position points are around northeast. When $P_t = 1000[W]$ which equal to the estimated power $P_{t_{ref}}$, the location with highest probability is very close to the true possible location identified by C4ADS which is marked by pink dot and that scenario has 92.6% probability of being true.

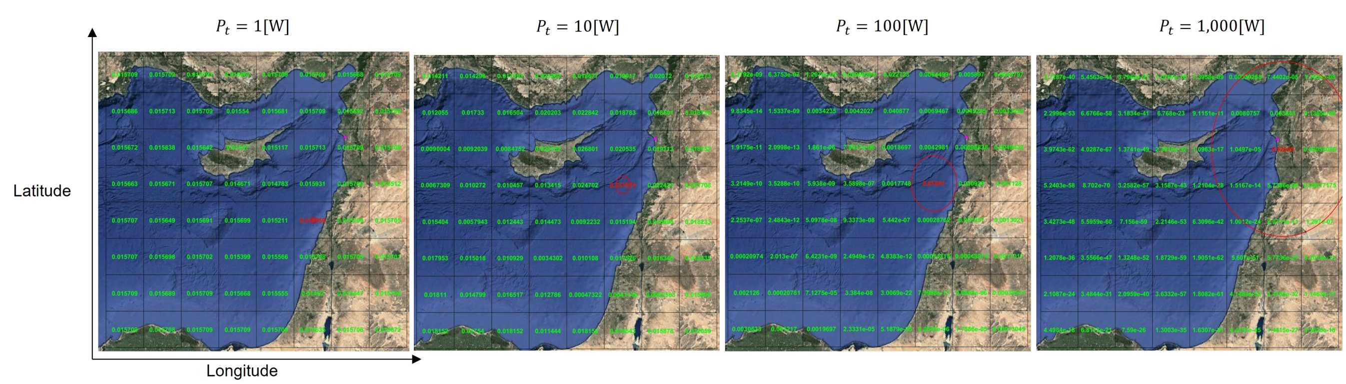

Figure 9: Probability of different scenarios

Figure10 shows the contour plot of above probabilities. Noticed that as transmitted jamming power increases, the probability contours have more confidence about where the jammer could be. This is due to the fact that more points can be enclosed by jammer impact region which provides more effective information.

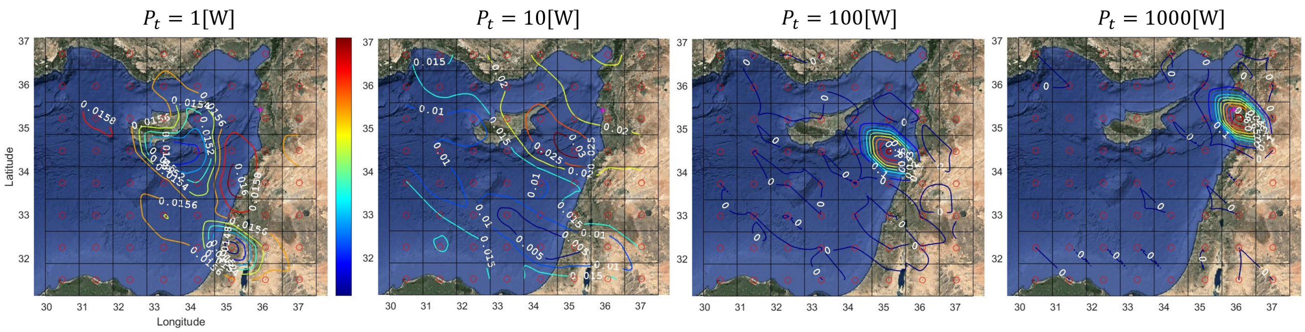

Figure 10: Contour of probabilities for different scenarios

Therefore, our algorithm provides a quite reasonable solution for real interference event. The only concern is that in current airspace, due to the lack of coverage from publicly accessible data, most of the data we collected was from southwest side of the jammer. This imbalanced data distribution might leads to some biased prediction. We need to test our models in other airspace where ADS-B data can be collected evenly from all directions to the interference source.

2. Simulated cases

Since it is difficult to find real-world ADS-B data which has a known jammer location and an adequate density of points in all directions about the jammer, we built a simulator to generate ADS-B data based on selected type of interference event. Figure 12 shows top view of simulated air traffic. Here we are simulating an interference event cause by a jammer located at the center of the airspace with $P_t = 1000$[W]. Notice that some areas are empty, this is the result of mimicking cases where no ADS-B data is received due to the lack of ground coverage of receiver. In addition, sometimes we will randomly add in some flights with NIC always equal to zero during simulation. This is a case we observed during investigation of real interference events, which is caused by incorrect operation of the on-board ADS-B system.

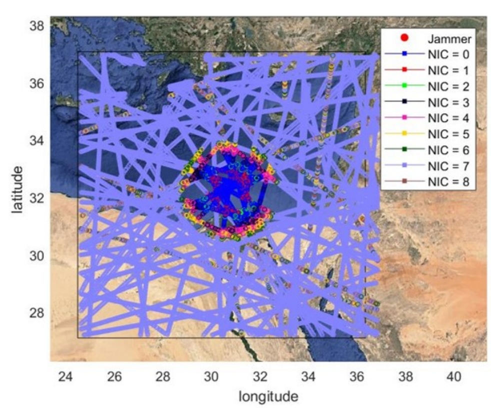

Figure 11: Top view of air traffic within simulated airspace

This time, instead of showing probability result for each power level separately, we will show the direct result from the algorithm. Our approach considers all possible power level at each location and returns the local maximum probability value as well as the corresponding P_t value. The algorithm then compares among probabilities at different locations and shows 99% probability of the jammer locating at the center of the airspace with $P_t \approx 1000$[W]. This result matches exactly with the true information of jammer as expected.

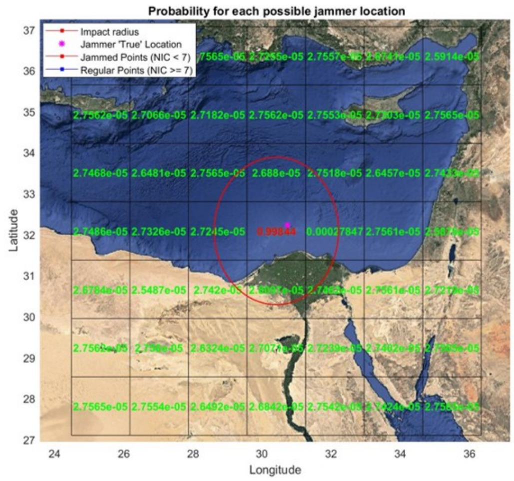

Figure 12: Highest probability of different scenarios at each location

V. CONCLUSION

This project designed and showed possible approach for interference source localization using ADS-B data. The result shows that this approach can perform reasonably well for single-jammer with any possible power levels.

As for future work, we could easily extend current model to solve multi-jammer problem, by adding one more searching dimension corresponding to different numbers of jammers. More real-world data is desired for further testing and validating on our models, especially reported interference event with information about the true location of the jammer. Improving the robustness and accuracy of our current approaches is another future work, such as designing an algorithm to determine whether a position point has truly been jammed. Also, we want to convert grid searching into continuous function which could evaluate best scenario using optimization methods.

ACKNOWLEDGEMENTS

We gratefully acknowledge the support of the FAA Satellite Navigation Team for funding this work under Memorandum of Agreement : 693KA8-19-N-00015. We also thank OpenSky Network for providing ADS-B data for this study.

REFERENCES

[1] M. Garcia, “Global surveillance and tracking of aircraft via satellite,” presented to SCPNT Symposium, Stanford University, CA, USA, October 28, 2020. [*PowerPoint* slides]. Available at http://web.stanford.edu/group/scpnt/pnt/PNT20/presentation_files/Day2-6-Garcia.pdf.

[2] P. Barret, G. Berz, P. Salabert, and K. Ashton, “Eurocontrol gnss research update,” presented to CGSIC 2016–International Session, OR, Portland, September 12, 2016. [*PowerPoint* slides]. Available at https://www.gps.gov/cgsic/meetings/2016/berz.pdf.

[3] Z. Liu, S. Lo, and T. Walter, “Characterization of ads-b performance under gnss interference,” *Proceedings of the 33rd International Technical Meeting of the Satellite Division of The Institute of Navigation (ION GNSS+ 2020)*, pp. 3581–3591, September 2020.

[4] Office of the Federal Register, National Archives and Records Administration, *14 CFR § 91.227 - Automatic Dependent Surveillance-Broadcast (ADS-B) Out equipment performance requirements*. [Government]., 2013, December 31.

[5] M. Schäfer, M. Strohmeier, V. Lenders, I. Martinovic, and M. Wilhelm, “Bringing up opensky: A large-scale ads-b sensor network for research,” in *ACM/IEEE International Conference on Information Processing in Sensor Networks*, April 2014.

[6] P. Jonáš and V. Vitan, “Detection and localization of gnss radio interference using ads-b data,” in *2019 International Conference on Military Technologies (ICMT)*, 2019, pp. 1–5.

[7] Z. Liu, S. Lo, and T. Walter, “Gnss interference characterization and localization using opensky ads-b data,” *Proceedings*, vol. 59, p. 10, 12 2020.

[8] DO-260B RTCA (Firm), *Minimum Operational Performance Standards (MOPS) for 1090 MHz Extended Squitter Automatic Dependent Surveillance-Broadcast (ADS-B) and Traffic Information Services-Broadcast (TIS-B)*. Washington, DC, USA: RTCA, 2011.

[9] H. T. Friis, “A note on a simple transmission formula,” *Proceedings of the IRE*, vol. 34, no. 5, pp. 254–256, 1946.

[10] EUROCONTROL, “Does radio frequency interference to satellite navigation pose an increasing threat to network efficiency, cost-effectiveness and ultimately safety?” presented to Aviation Intelligence Unit, Think Paper 9, March 01, 2021. [*PowerPoint* slides]. Available at https://www.eurocontrol.int/sites/default/files/2021-03/eurocontrol-think-paper-9-radio-frequency-intereference-satellite-navigation.pdf.

[11] Center for Advanced Defense Studies, *Above Us Only Stars: Exposing GPS Spoofing in Russia and Syria*. Washington, DC: C4ADS, 2019.

[12] E. Kaplan and C. Hegarty, *Understanding GPS/GNSS: Principles and Applications*, 3rd ed. Artech, 2017.